Salaheddin Zabalawi
Josh Zagorski
Advanced Linear Systems Analysis Term Project

Simulation of Respiratory Mechanics

RONALD W. JODAT, JAMES D. HORGAN, and RAMON L. LANGE

December 13th, 2007

UNIVERSITY of WISCONSIN
UWMILWAUKEE

Introduction

The authors of the paper aimed to describe the mechanical dynamics of a single breath. The authors achieved this by deriving the system's mathematical model that consists of three differential equations and simulating them with a computer. We extended their approach by modeling the system using state space modeling.

The mechanical dynamics are just one aspect of the respiratory system, Fig. 1. In order to completely simulate the complete respiratory system, the chemical, biological, mechanical, and control dynamics of the system need to be considered. The approach of this paper is to convert the muscle effort controlled by the respiratory control center and converts it to lung volume.

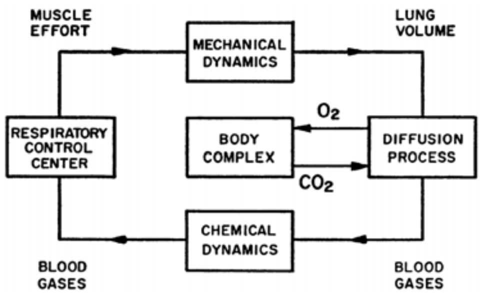

Figure 1: Complete Respiratory System

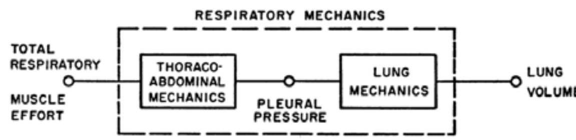

Figure 2: Breakdown of the Mechanical Dynamics

The authors claim that a highly accurate respiratory model is achievable by mechanically interconnecting parameters of mass, compliance, and viscous resistance for each structure. Fig. 2 breaks down the Mechanical Dynamics block even further to physical dynamics of the thoracoabdominal muscle mechanics and their effect on the pleural cavity pressure. From the pleural cavity pressure we can formulate its effect on the lung volume. Fig. 3 shows the conversion from the biological system to a mechanical representation of the constituent components.

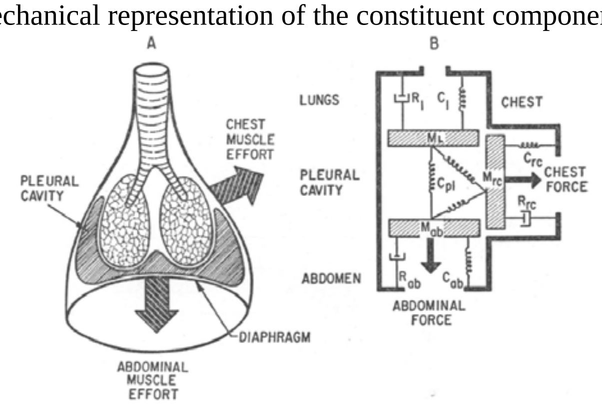

Figure 3: Anatomical to Mechanical Model

Mathematical Derivation

The mechanical representation in Fig. 3 is then converted to the system model shown in Fig. 4, with two inputs; abdominal muscle pressure and chest muscle pressure, and one output; lung volume.

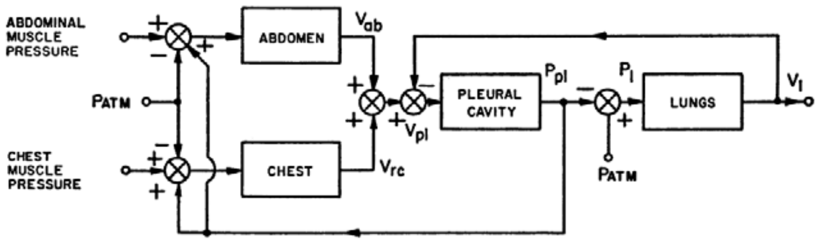

Figure 4: Full System Model

The blocks in Fig. 4 give three second order differential equations along with the linear relationship between the pleural pressure and the volume of the chest, lungs, and abdomen. The second order equations are shown below:

Lungs

$$M_l \ddot{V}_l + R_l \dot{V}_l + \frac{V_l}{C_l} = P_{ATM} - P_{pl}$$

Abdomen

$$M_{ab} \ddot{V}_{ab} + R_{ab} \dot{V}_{ab} + \frac{V_{ab}}{C_{ab}} = P_{mus(ab)} + P_{pl} - P_{ATM}$$

Rib Cage

$$M_{rc} \ddot{V}_{rc} + R_{rc} \dot{V}_{rc} + \frac{V_{rc}}{C_{rc}} = P_{mus(rc)} + P_{pl} - P_{ATM}$$

Pleural Cavity

$$P_{pl} = \frac{V_{pl}}{C_{pl}} = \frac{V_{rc} + V_{ab} - V_l}{C_{pl}}$$

Rearranging and combining the equations gives the three second order differential equations in the form shown below. We can convert them into a sixth order state space model seen in Fig. 5. The A, B, C, and D matrices of which can be seen in Fig. 6.

$$\ddot{V}_l = -\frac{R_l \dot{V}_l}{M_l} - \frac{V_l}{M_l C_l} - \frac{V_{rc} + V_{ab} - V_l}{M_l C_{pl}} + \frac{P_{ATM}}{M_l}$$

$$\ddot{V}_{rc} = -\frac{R_{rc} \dot{V}_{rc}}{M_{rc}} - \frac{V_{rc}}{M_{rc} C_{rc}} + \frac{V_{rc} + V_{ab} - V_l}{M_{rc} C_{pl}} + \frac{P_{mus(rc)} - P_{ATM}}{M_{rc}}$$

$$\ddot{V}_{ab} = -\frac{R_{ab} \dot{V}_{ab}}{M_{ab}} - \frac{V_{ab}}{M_{ab} C_{ab}} + \frac{V_{rc} + V_{ab} - V_l}{M_{ab} C_{pl}} + \frac{P_{mus(ab)} - P_{ATM}}{M_{ab}}$$

$$\begin{bmatrix} \ddot{V}_l \\ \dot{V}_l \\ \ddot{V}_{rc} \\ \dot{V}_{rc} \\ \ddot{V}_{ab} \\ \dot{V}_{ab} \end{bmatrix} = A \begin{bmatrix} \dot{V}_l \\ V_l \\ \dot{V}_{rc} \\ V_{rc} \\ \dot{V}_{ab} \\ V_{ab} \end{bmatrix} + B \begin{bmatrix} P_{atm} \\ P_{mus(rc)} \\ P_{mus(ab)} \end{bmatrix} \qquad V_l = C \begin{bmatrix} \dot{V}_l \\ V_l \\ \dot{V}_{rc} \\ V_{rc} \\ \dot{V}_{ab} \\ V_{ab} \end{bmatrix} + D \begin{bmatrix} P_{ATM} \\ P_{mus(rc)} \\ P_{mus(ab)} \end{bmatrix}$$

Figure 5: 6th Order State Space Model

$$A=\begin{bmatrix} -\frac{R_l}{M_l} & \frac{1}{M_lC_{pl}}-\frac{1}{M_lC_l} & 0 & -\frac{1}{M_lC_{pl}} & 0 & -\frac{1}{M_lC_{pl}} \\ 1 & 0 & 0 & 0 & 0 & 0 \\ 0 & -\frac{1}{M_{rc}C_{pl}} & -\frac{R_{rc}}{M_{rc}} & \frac{1}{M_{rc}C_{pl}}-\frac{1}{M_{rc}C_{pl}} & 0 & \frac{1}{M_{rc}C_{pl}} \\ 0 & 0 & 1 & 0 & 0 & 0 \\ 0 & -\frac{1}{M_{ab}C_{pl}} & 0 & \frac{1}{M_{ab}C_{pl}} & -\frac{R_{ab}}{M_{ab}} & \frac{1}{M_{ab}C_{pl}}-\frac{1}{M_{ab}C_{ab}} \\ 0 & 0 & 0 & 0 & 1 & 0 \end{bmatrix}$$

$$B=\begin{bmatrix} \frac{1}{M_l} & 0 & 0 \\ 0 & 0 & 0 \\ -\frac{1}{M_{rc}} & \frac{1}{M_{rc}} & 0 \\ 0 & 0 & 0 \\ -\frac{1}{M_{ab}} & 0 & \frac{1}{M_{ab}} \\ 0 & 0 & 0 \end{bmatrix} \qquad \begin{aligned} C &= [0 \quad 1 \quad 0 \quad 0 \quad 0 \quad 0] \\ D &= [0] \end{aligned}$$

Figure 6: State Space Variables

Simplifications

The authors performed their analysis on an IBM 1620 computer in 1966. To make the system less computationally intense, four simplifications were made to bring the system down from a sixth order system to a third order system. A fifth simplification was also included to make the system and single input single output system (SISO). The simplifications are as follows:

1. Use the atmospheric pressure at sea level as a zero reference point.
2. Pleural Space is stiff (very low compliance structure).
3. Mass terms are negligible compared to viscous and elastic terms.
4. All parameters are considered linear and time invariant
5. Combine the muscle pressures $P_{mus(rc)}$ and $P_{mus(ab)}$ into a single driving force P_M.as seen in Fig. 8-10.

The system's first order equations will be:

Pleural Cavity

$$P_{pl}=\frac{V_{pl}}{C_{pl}}=\frac{V_{rc}+V_{ab}-V_l}{C_{pl}}$$

Chest

$$\dot{V}_{rc}=-\frac{V_{rc}}{R_{rc}C_{pl}}+\frac{V_{rc}+V_{ab}-V_l}{R_{rc}C_{pl}}+\frac{P_{mus(rc)}}{R_{rc}}$$

Lungs

$$\dot{V}_l=-\frac{V_l}{R_lC_l}-\frac{V_{rc}+V_{ab}-V_l}{R_lC_{pl}}$$

Abdomen

$$\dot{V}_{ab}=-\frac{V_{ab}}{R_{ab}C_{ab}}+\frac{V_{rc}+V_{ab}-V_l}{R_{ab}C_{pl}}+\frac{P_{mus(ab)}}{R_{ab}}$$

$$\begin{bmatrix}\dot{V}_l \\ \dot{V}_{rc} \\ \dot{V}_{ab}\end{bmatrix}=\begin{bmatrix} \frac{1}{R_lC_{pl}}-\frac{1}{R_lC_l} & -\frac{1}{R_lC_{pl}} & -\frac{1}{R_lC_{pl}} \\ -\frac{1}{R_{rc}C_{pl}} & \frac{1}{R_{rc}C_{pl}}-\frac{1}{R_{rc}C_{rc}} & \frac{1}{R_{rc}C_{pl}} \\ -\frac{1}{R_{ab}C_{pl}} & \frac{1}{R_{ab}C_{pl}} & \frac{1}{R_{ab}C_{pl}}-\frac{1}{R_{ab}C_{ab}} \end{bmatrix}\begin{bmatrix}V_l \\ V_{rc} \\ V_{ab}\end{bmatrix}+\begin{bmatrix} 0 & 0 \\ \frac{1}{R_{rc}} & 0 \\ 0 & \frac{1}{R_{ab}} \end{bmatrix}\begin{bmatrix}P_{mus(rc)} \\ P_{mus(ab)}\end{bmatrix}$$

Figure 7: 3rd Order State Space Model

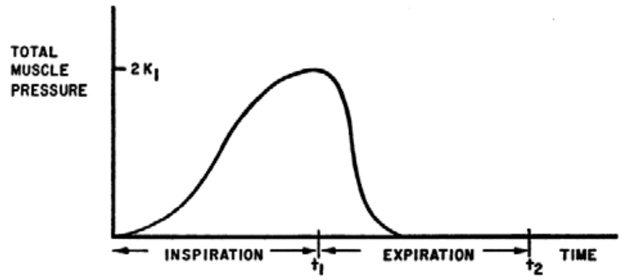

Figure 8: Muscle Pressure Driving Function

$$\begin{bmatrix} P_{mus(rc)} \\ P_{mus(ab)} \end{bmatrix} = \begin{bmatrix} K_2 \\ 1-K_2 \end{bmatrix} P_M \text{, where } P_M = \begin{cases} K_1[1-\cos(\alpha_1 t); & 0 < t \le t_1 \\ K_1[1-\cos(\alpha_2 t - \alpha_1 t_1); & t_1 < t \le t_2 \end{cases}$$

$$\alpha_1 < \alpha_2$$

Figure 9: System Input

Combining Fig. 7-9, we can construct the following new state space model.

$$\begin{bmatrix} \dot{V}_l \\ \dot{V}_{rc} \\ \dot{V}_{ab} \end{bmatrix} = \begin{bmatrix} \frac{1}{R_l C_{pl}} - \frac{1}{R_l C_l} & -\frac{1}{R_l C_{pl}} & -\frac{1}{R_l C_{pl}} \\ -\frac{1}{R_{rc} C_{pl}} & \frac{1}{R_{rc} C_{pl}} - \frac{1}{R_{rc} C_{rc}} & \frac{1}{R_{rc} C_{pl}} \\ -\frac{1}{R_{ab} C_{pl}} & \frac{1}{R_{ab} C_{pl}} & \frac{1}{R_{ab} C_{pl}} - \frac{1}{R_{ab} C_{ab}} \end{bmatrix} \begin{bmatrix} V_l \\ V_{rc} \\ V_{ab} \end{bmatrix} + \begin{bmatrix} 0 \\ \frac{K_2}{R_{rc}} \\ \frac{1-K_2}{R_{ab}} \end{bmatrix} P_M$$

Figure 10: State Space with P_M

Functional Relationship

During a breath, the chest muscles only have a fixed volume to which they can inflate and the abdominal muscles need to take over, see Fig. 14. The authors refer to this as the functional relationship. The equations of the functional relationship are given below. This adds a new component to the system model, see Fig. 12.

Inspiration Expiration

$$P_{FR} = \begin{cases} P_{MA}; & P_{MA} \le K_3 \\ K_3; & P_{MA} \ge K_3 \end{cases} \qquad P_{FR} = \begin{cases} K_3 - P_{MAX} - P_{MA}; & P_{MAX} - P_{MA} \le K_3 \\ 0; & P_{MAX} - P_{MA} \ge K_3 \end{cases}$$

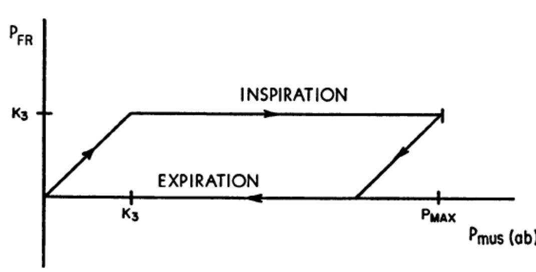

Figure 11: Functional Relationship

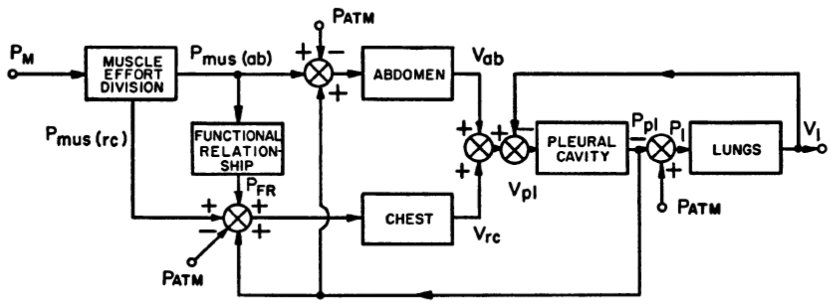

Figure 12: System Model with Functional Relationship

In order to perform an accurate simulation that includes the functional relationship block, we need to write down the state space model with three inputs. The new inputs will be called P_{ab} and P_{rc} and they are the signals entering the abdominal block and rib cage block respectively.

We will make the following substitutions:

$$P_{ab} = P_{mus(ab)} - P_{ATM} + P_{Pl} \Rightarrow P_{mus(ab)} = P_{ab} - P_{Pl}$$
$$P_{rc} = P_{FR} + P_{mus(rc)} - P_{ATM} + P_{Pl} \Rightarrow P_{mus(rc)} = P_{rc} - P_{FR} - P_{Pl}$$

The final state space model will be:

$$\begin{bmatrix} \dot{V}_l \\ \dot{V}_{rc} \\ \dot{V}_{ab} \end{bmatrix} = \begin{bmatrix} \frac{1}{R_l C_{pl}} - \frac{1}{R_l C_l} & -\frac{1}{R_l C_{pl}} & -\frac{1}{R_l C_{pl}} \\ 0 & -\frac{1}{R_{rc} C_{rc}} & 0 \\ 0 & 0 & -\frac{1}{R_{ab} C_{ab}} \end{bmatrix} \begin{bmatrix} V_l \\ V_{rc} \\ V_{ab} \end{bmatrix} + \begin{bmatrix} 0 & 0 & 0 \\ -\frac{1}{R_{rc}} & \frac{1}{R_{rc}} & 0 \\ 0 & 0 & \frac{1}{R_{ab}} \end{bmatrix} \begin{bmatrix} P_{FR} \\ P_{rc} \\ P_{ab} \end{bmatrix}$$

$$y = [1 \quad 0 \quad 0] \begin{bmatrix} V_l \\ V_{rc} \\ V_{ab} \end{bmatrix}$$

Figure 13: 3rd Order State Space Model with FR

Both controllability and observability matrixes for this system matrix were built and found to have a third rank.

Simulink Simulation

The system model with functional relationship block was built and simulated using Simullink®.

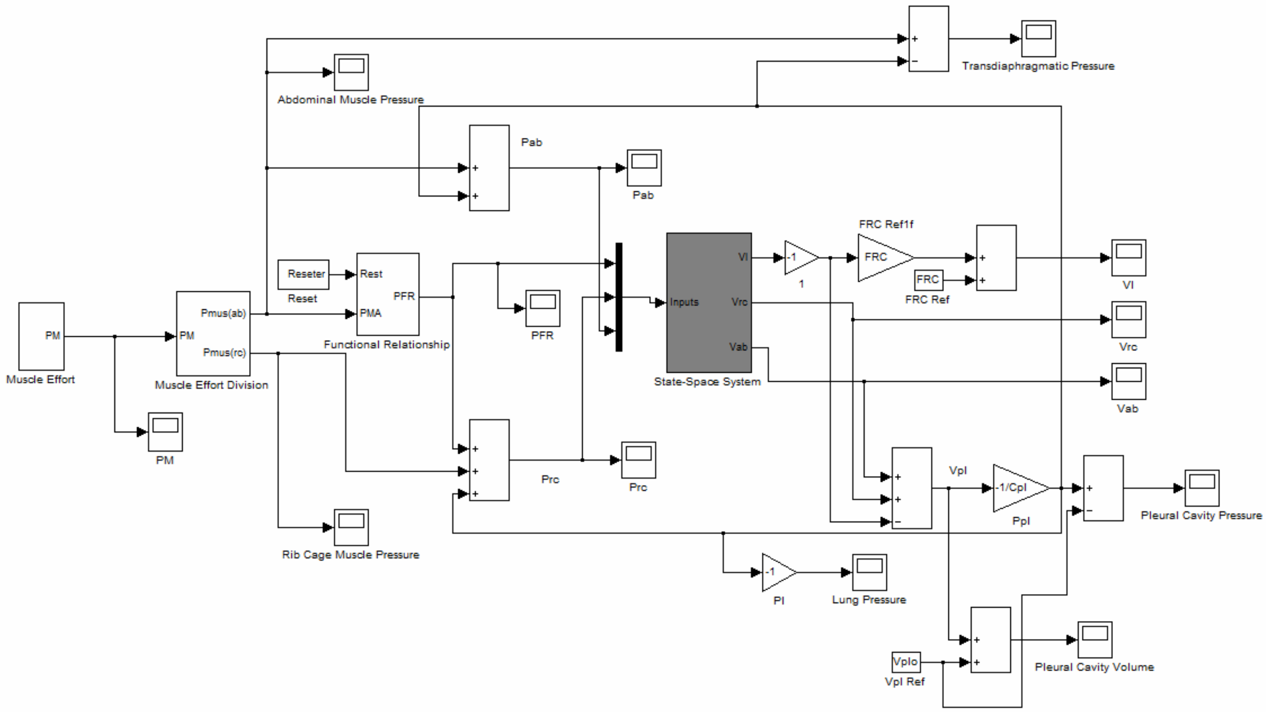

Figure 14: Simulink Simulation

The muscle effort block, shown in the previous figure, produces a single system input that exactly matches the driving function shown in Fig. 8.

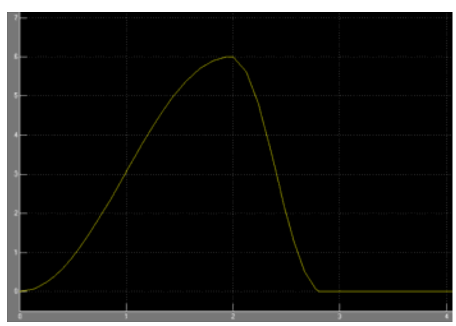

Figure 15: Simulated Driving Function

The driving function is then divided into two different functions, one is simulating the abdomen effort, $P_{mus(ab)}$, and another is simulating the rib cage effort, $P_{mus(rc)}$. Three different signals are resulting from the state space block; the lung, rib cage and abdomen volumes. Those volumes are added up and fed back to form the inputs of the system.

Different pressure signals produced in the system are observable through the scopes. Also, since not all volumes start from a zero value, some gain blocks were inserted to introduce a reference volume or pressure.

Simulation Results

To compare our system's results to the ones in the paper, we concentrated on three key signals, the lung volume, transdiaphragmatic and pleural pressures. For a healthy person, the simulation will run using the system parameters in table 1, the normal column. For the increased lung stiffness disorder, the system parameters in the third column are used (C_l changes from 0.2 to 0.1). For the increased air way resistance disorder, the system parameters in the fourth column are used (R_l changes from 2.0 to 10.0). The following figures show how we accurately reproduced the paper key waveforms. It is important to note that since we are using 0.55 for Pleural Cavity Compliance instead of 0.005, the magnitude of some waveforms is not exactly matching the magnitude of the waveforms in the paper. Therefore, we concentrated on the waveforms shapes more than their magnitudes.

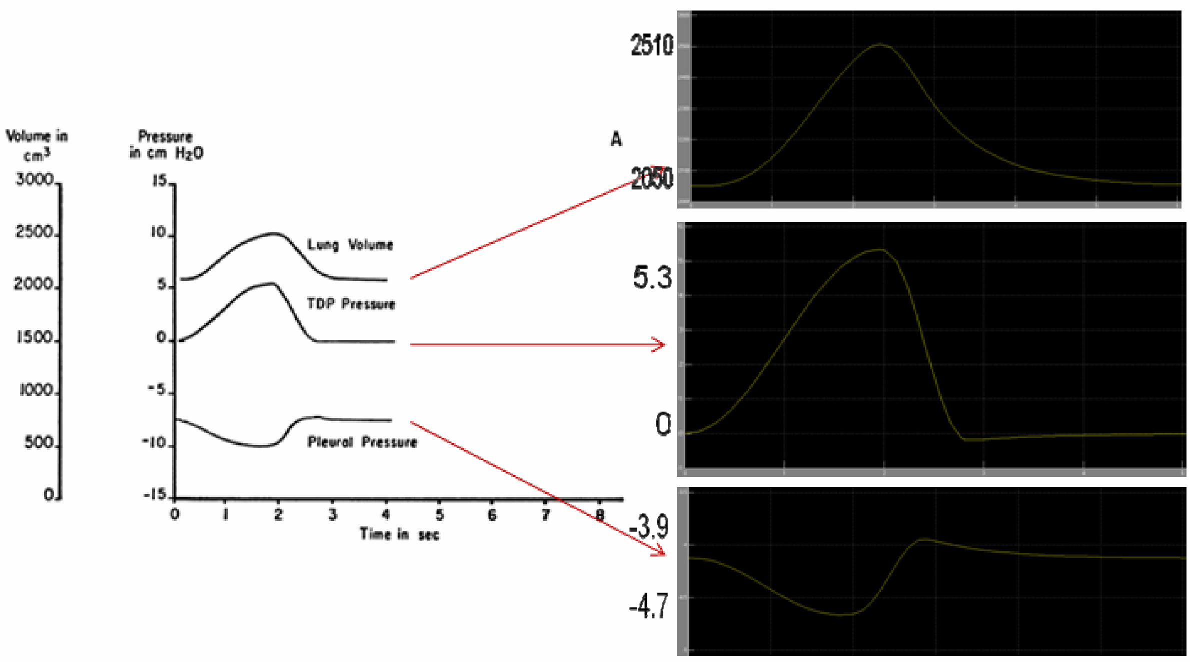

Figure 16: Waveforms for a healthy person

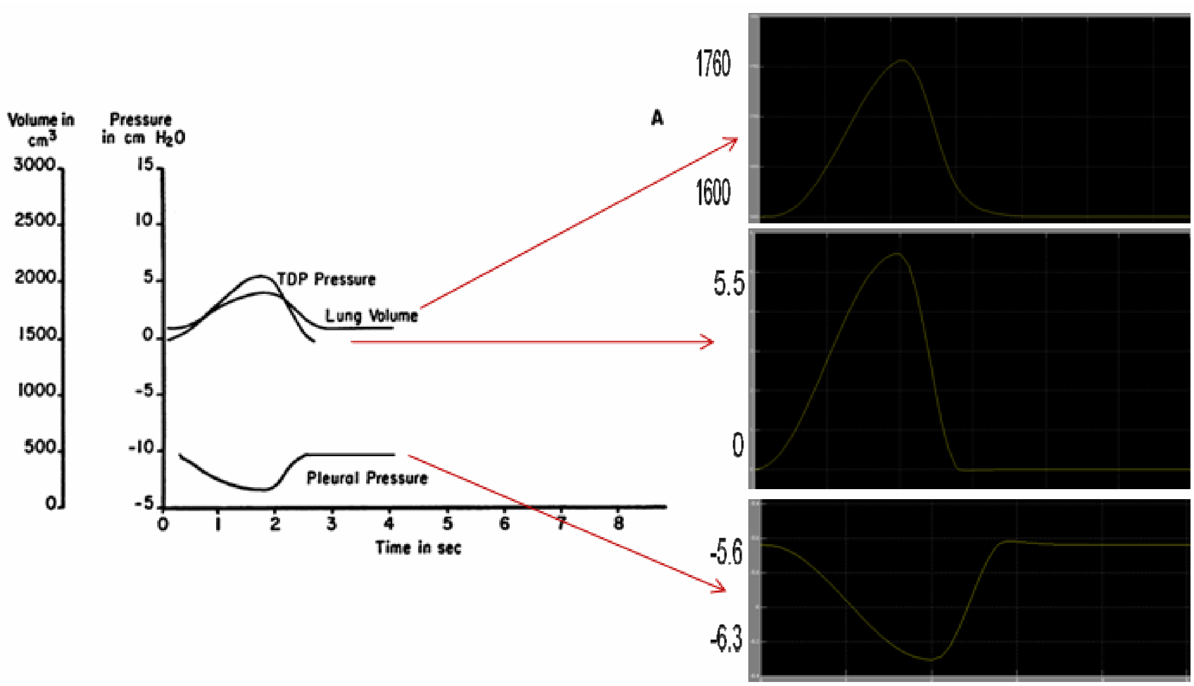

Figure 17: Waveforms for increased lung stiffness

Comparing figure 16 with 17, we can see how decreasing lung compliance (Cl) causes an increase in the pleural pressure (Ppl) magnitude.

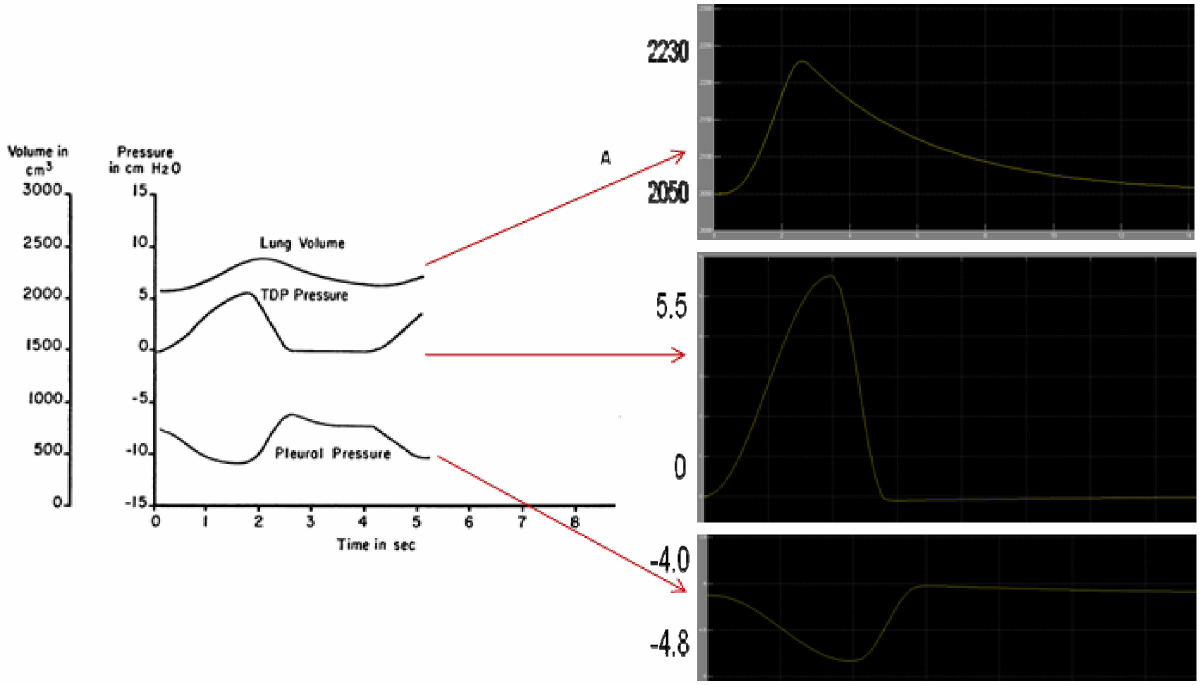

Figure 18: Waveforms for increased airway resistance

Comparing figure 16 with 18, we can see how increasing lung damping (R_l) causes, approximately, no change to pleural pressure. Pleural pressure rapidly increases with little decrease in lung volume.

Discussion

We were able to verify the authors' main results and conclusions they drew from their simulation. First of all, the lung always expands only under greater negative pleural pressure. In other words, when the plural pressure goes more into a negative value, the lung volume increases and vice versa.

In both abnormal states, the transdiaphragmatic pressure has an additional increase in magnitude to bring the tidal volume up to normal. Also, in both pulmonary disorders, the pleural pressure range increases and the abdominal pressure variation decreases. Additionally, we can note that the maximum inspiratory and expiratory flow rates become the same for the case of increased lung damping (R_l). Finally, a decrease in lung compliance does not greatly affect the difference between the maximum inspiratory and expiratory flow rates (their individual magnitudes become smaller, but their difference is approximately the same).

Conclusion

In conclusion, we were able to use the system's differential equations for state space modeling. The proposed state space model produced the same waveforms produced by the author's set of differential equations. State space modeling was not a straight forward approach in our application. We had to modify the system inputs to be able to take into account the effect of the functional relationship block. Moreover, the system was not stable at the beginning; producing the

Eigen values of the system matrix used to show positive Eigen values. After some investigation, we found that one of the approximations the authors used in their design is not valid when constructing the state space model of the system. Their second simplification or approximation in which they assumed the pleural cavity compliance should be very small was causing the instability. Therefore, we changed the 0.0005 value to 0.55. We do not really acknowledge the reason behind the second assumption, but we consider it as a weakness point in the paper.

We are convinced with the modeling and results shown in the paper. The produced waveforms agree with the literature. Even the waveforms that were produced for lung disorders agree with the clinical studies on patients having the same disorders.

In fact, this project was a very precious learning experience in which we had to study the state space modeling in depth and be able to solve a real problem that can arise in any design experience, the instability problem.

References

[1] Ronald W. Jodat, James D. Horgan, and Ramon L. Lange. Simulation of Respiratory Mechanics. Biophys J. 1966 November; 6(6): 773–785.

[2] Fundamentals of Linear State Space Systems, by J. S. Bay, McGraw Hill, 1999.

Appendix

Modified System Parameters

Parameter	Normal	Decreased Lung Compliance	Increased Lung Damping	Units
Abdominal Compliance	0.1	0.1	0.1	Liters/cm H_20
Chest Compliance	0.1	0.1	0.1	Liters/cm H_20
Lung Compliance	0.2	0.1	0.2	Liters/cm H_20
Pleural Cavity Compliance	0.55	0.55	0.55	Liters/cm H_20
Abdominal Damping	1	1	1	Cm H_20/(liters/s)
Chest Damping	1	1	1	Cm H_20/(liters/s)
Lung Damping	2	2	10	Cm H_20/(liters/s)
K1	3	3	3	Cm H_20
K2	0.2	0.2	0.2	None
K3	3	3	3	Cm H_20